PERGAMON

Applied Geochemistry 16 (2001) 1067–1082

Applied Geochemistry

www.elsevier.com/locate/apgeochem

The adsorption characteristics of δ-manganese dioxide: a collection of diffuse double layer constants for the adsorption of H^+, Cu^{2+}, Ni^{2+}, Zn^{2+}, Cd^{2+} and Pb^{2+}

P. Julius Pretorius [a,*], Peter W. Linder [b]

[a] *Division of Water, Environment and Forestry Technology, CSIR, PO Box 320, Stellenbosch 7599, South Africa*
[b] *Department of Chemistry, University of Cape Town, Rondebosch 7701, South Africa*

Received 21 September 1999; accepted 1 November 2000
Editorial handling by Z. Zhou

Abstract

Thermodynamic data for all fate-determining processes are needed in order to predict the fate and transport of metals in natural systems. The surface complexation properties of a synthetic MnO_2, δ-MnO_2, have accordingly been investigated using glass electrode potentiometry. Experimental data were interpreted according to the surface complexation model in conjunction with the diffuse double layer model of the solid/solution interface. Adsorption constants were determined using the non-linear optimisation program FITEQL. Surface complexation parameters determined in this way were validated against results obtained from the literature. Best fits of alkalimetric titration data were obtained with a 2-site, 3 surface-species model of the δ-MnO_2 surface. Site concentrations of 2.23×10^{-3} mol g^{-1} and 7.66×10^{-4} mol g^{-1} were obtained. Corresponding logarithms of formation constants for the postulated surface species are -1.27 ($\equiv XO^-$), -5.99 ($\equiv YO^-$) and 3.52 ($\equiv YOH_2^+$) at I = 0.1 M. The surface speciation of δ-MnO_2 is dominated by $\equiv XO^-$ over the pH range investigated. Metal adsorption was modelled with surface species of the type $\equiv XOM^+$, $\equiv XOMOH$, $\equiv YOM^+$, $\equiv YOMOH$ (M = Cu, Ni, Zn, Cd and Pb) and $\equiv XOM_2OH^{2+}$ (M = Pb). For Cu, Ni and Zn, titration data could be modelled with $\equiv XOM^+$, $\equiv XOMOH$, $\equiv YOM^+$ and $\equiv YOMOH$, whereas for Cd, $\equiv XOM^+$ and $\equiv YOM^+$ were sufficient. Lead data were best modelled by assuming the dinuclear species $\equiv XOM_2OH^{2+}$ to be the only surface species to form. Adsorption constants determined for Ni, Cu and Zn follow the Irving-Williams sequence. The model suggests an adsorption order of (Pb, Cu) > (Ni, Zn) > Cd. The discrepancy between model predictions and published adsorption results is similar to the variability observed in experimental results from different laboratories.

1. Introduction

The fate and transport of trace metals in natural systems are, to a large extent, influenced by adsorption onto colloidal particles such as the oxides of Fe, Mn and Al as well as particulate organic matter (Lyman, 1995; Ure and Davidson, 1995). Evidence indicates that the biological effects of metals in soil and sedimentary systems are related to concentrations prevalent in pore waters instead of total solid phase metal concentration (Adams et al., 1992). The concept of equilibrium partitioning (Shea, 1988) is commonly used to predict solution phase concentrations from total solid phase concentrations. A problem with the application of this is that the partition coefficient, K_D, is a function of both metal speciation and the factors controlling metal speciation (van der Kooij et al., 1991). Chemical equilibrium modelling has long been used for the modelling of metal speciation in the environment (Waite, 1989; Bassett and Melchior, 1990). However, a difficulty with the

* Corresponding author at current address: Sasol Technology, PO Box 1, Sasolburg 1947, South Africa. Fax: +27-16-960-2826.
E-mail address: julius.pretorius@sasol.com (P.J. Pretorius).

0883-2927/01/$ - see front matter
PII: S0883-2927(01)00011-7

application of this technique to natural systems is the representation of the interaction of metals with heterogeneous environmental materials, such as the humic materials and the surfaces of colloidal particles (Westall et al., 1995).

Moreover, sorption constants are expressed using different models of the solid/solution interface. These models are based on the same concepts but assume different physical-chemical configurations for ions sorbed at the mineral/water interface. As a result, somewhat different parameter values are obtained and parameters that are common among the models are not directly comparable (Dzombak and Hayes, 1992), resulting in sorption constants that are not inter-convertible. This situation has impeded the inclusion of surface complexation in chemical equilibrium modelling of natural systems. In an attempt to overcome this, Dzombak and Morel (1990) published a consistent set of Diffuse double layer adsorption constants for metal sorption by hydrous ferric oxides (HFO). This data compilation has been included in the MINTEQA2 speciation programme (Allison et al., 1991). However, for other important phases, such as MnO_2 (Morgan and Stumm, 1964; McKenzie, 1989; Onuki, 1990), adsorption constants compatible with the HFO data are not available. Few studies aimed at measuring surface complexation constants for this solid have been reported (e.g. Catts and Langmuir, 1986; Fu et al., 1991; Smith and Jenne, 1991). These studies report adsorption constants based on the triple layer model.

In this paper the authors describe the surface chemistry of δ-MnO_2 with respect to H^+, Ni^{2+}, Cu^{2+}, Zn^{2+}, Cd^{2+} and Pb^{2+}. Surface complexation parameters (binding site concentrations and diffuse double layer surface complexation constants) are presented that allow the inclusion of this solid phase in the general chemical equilibrium framework. The utility of this set of parameters for the prediction of independently collected sorption data is also assessed.

2. Materials and methods

2.1. Synthesis and characterisation of δ-MnO_2

Manganese dioxide was prepared according to the 'redox' method outlined by Stroes-Gascoyne et al. (1987). Manganese dioxide forms according to the reaction

$$3Mn^{2+} + 2MnO_4^- + 2H_2O \rightleftharpoons 5MnO_2 + 4H^+.$$

δ-MnO_2 was prepared by dissolving 5.2 g $Mn(NO_3)_2.4H_2O$ (SAARCHEM, AR) in 900 cm^3 deionised, glass-distilled water. To this, 100 cm^3 of a solution of 2.2g $KMnO_4$ (May and Baker) and 1.6 g KOH (SAARCHEM, AR) was added from a fast dripping burette. A dark brown to black precipitate formed immediately and the solution was stirred continuously for 1 h. Stirring was discontinued and the suspension was allowed to settle (ca. 30 min). Excess supernatant was removed and the concentrated suspension was transferred to glass centrifuge tubes and centrifuged for 20 min. The supernatant was decanted, and the residue resuspended with distilled water. This process was continued until a supernatant conductivity smaller than that of a solution of 1×10^{-4} M KNO_3 was observed. The suspension was washed into a round bottom flask with distilled water and stored with continuous stirring, using a Teflon coated magnetic stirrer bar. A solids concentration of 1.75 ± 0.01 g dm^{-3} was determined by evaporation of accurately measured aliquots of the suspension.

N_2-BET surface area of 331 m^2 $g^{-1}$was obtained for the solid. This corresponds well with values reported by Fu et al. (1991), Catts and Langmuir (1986) and Stroes-Gascoyne et al. (1987). The shape of the gas adsorption isotherms together with the marked hysteresis exhibited is indicative of capillary condensation taking place in mesopores ranging from 2 to 50 nm in width (Sing, 1985). This is consistent with the idea that δ-MnO_2 is a porous solid (Manceau, 1992a,b). Powder X-ray diffraction analysis (CuK_α, $\lambda = 1.542$ Å) exhibited peaks at $d = 2.44$ Å and $d = 1.44$ Å (Fig. 1), which are typical of δ-MnO_2 (McKenzie, 1989).

2.2. Potentiometric titrations

Titrations of 20.0 cm^3 aliquots of suspension were conducted in a jacketed Pyrex vessel using a computer controlled Metrohm Dosimat 665 automatic burette. EMF was monitored with a radiometer pHM 64 pH meter. Glass electrodes (radiometer) were calibrated in terms of H^+ concentration using an internal calibration scheme (Linder et al., 1984). A titration of 20.0 cm^3 supernatant, collected over a 0.22 μm membrane filter (Millipore) was performed under conditions identical to those employed for the suspensions. Titrations were conducted in the presence 0.1 M KNO_3 (Merck, GR) as background electrolyte at 25°C with an initial solids concentration of 1.40 g dm^{-3}. An inert atmosphere was maintained by a constant flow of humidified, high purity N_2 gas. The suspension was titrated with standardised 0.1 M KOH solution (Merck Titrisol) containing 0.1 M KNO_3 (Merck, GR) background electrolyte. KOH was prepared under N_2 using de-aerated glass-distilled water. The solution was stored in a polyethylene vessel fitted with a Carbosorb CO_2 trap and attached to a Dosimat exchange unit. KOH was added in 0.02 cm^3 increments once EMF drift was less than 0.2 mV per 600 s or after 1200 s (20 min), whichever condition was satisfied first. Total H^+ concentration, T_H, at each titration point, i, was calculated using Eq. (1):

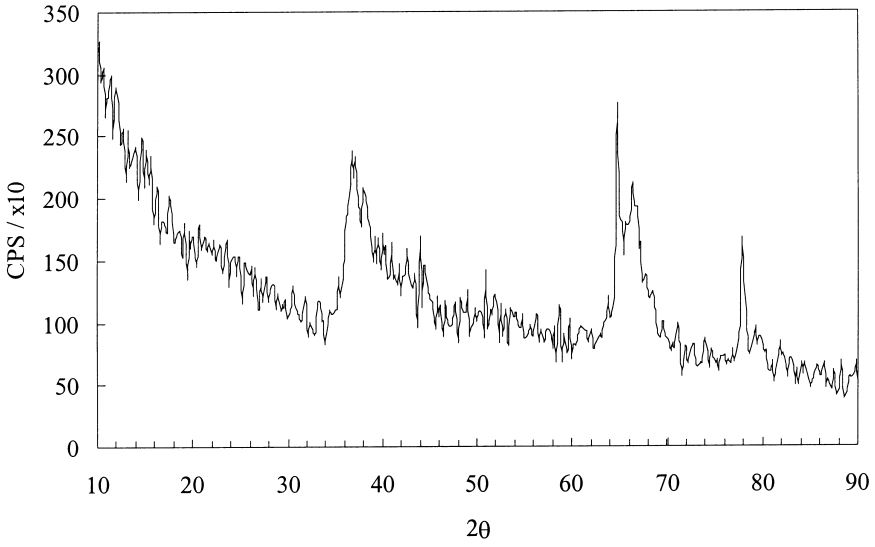

Fig. 1. X-ray diffraction pattern for the δ-MnO_2 solid used in this study.

$$T_{Hi} = \frac{(C_{acid} V_{acid}) - \left\{(C_{base} v_i) + \frac{K_w}{[H^+]}\right\}}{V_0 + v_i} \quad (1)$$

where C_{acid} is the molar concentration of excess acid (0.1 M HNO_3, Merck Titrisol) added at the start of the titration, C_{base} is the molar concentration of base, V_{acid} is the volume of excess acid added at the start of the titration, V_0 is the initial volume of suspension and v_i is the volume alkali added at each titration point. Surface charge density was determined by calculating the difference in $[H^+]$ between the supernatant and suspension titration curves for a given T_H using Eq. (2):

$$[\equiv SO^-] - [SOH_2^+] = [H^+]_{susp,i} - \frac{K_w}{[H^+]_{susp,i}} - [H^+]_{supn,i} + \frac{K_w}{[H^+]_{supn,i}} \quad (2)$$

where $[\equiv SO^-]$ and $[\equiv SOH_2^+]$ refer to the concentration of deprotonated and protonated sites respectively, K_w is the dissociation product of water, $[H^+]_{susp,i}$ and $[H^+]_{supn,i}$ refer to the H^+ concentration at titration point i in the presence and absence of δ-MnO_2 respectively. At high pH, $[\equiv SOH_2^+] \approx 0$, allowing the total concentration of titratable surface sites to be estimated. The surface site concentration of 4.1×10^{-3} M at pH 11 corresponds to a site density of approximately 6 sites nm^{-2}, which is in the range commonly reported for oxyhydroxides (Schindler and Stumm, 1987). It is slightly lower than the 8.1 sites nm^{-2} reported by Fu et al. (1991) and substantially lower than the values of 18 to 21 sites nm^{-2} obtained from tritium exchange studies (Balistrieri and Murray, 1982; Catts and Langmuir, 1986). The surface charge density of −66 μC cm^{-2} at pH 8, is comparable with the value of −50 μC cm^{-2} found by Catts and Langmuir at this pH and I = 0.1 M.

2.3. Adsorption constant determination

Protonation constants were determined from the potentiometric titration data using the non-linear optimisation program FITEQL (Herbelin and Westall, 1994). FITEQL is an iterative optimisation program that allows the optimisation of a number of specified parameters. Input data consisted of (a) total H^+ concentration, T_H, (M), (b) the logarithm of free H^+ concentration, $\log[H^+]$, (c) dilution factors and (d) mass of solid (g dm^{-3}). Surface protonation constants and surface site concentration were calculated from these data.

Input data for metal adsorption constant determination consisted of (a) total H^+ concentration, T_H, (M), (b) the logarithm of free H^+ concentration, $\log[H^+]$, (c) dilution factors, (d) mass of solid (g dm^{-3}), (e) binding site concentration (M), (f) surface protonation constants, (g) metal solution phase reactions and accompanying equilibrium constants and (h) total metal concentration, T_M. Here, adsorption constants were the only parameters that were optimised. Total binding site concentration and protonation constants were fixed at the values obtained from the protonation study. Equilibrium constants for solution phase reactions were corrected to an ionic strength of 0.1 M, using MINTEQA2 (Allison et al., 1991). Solution reactions and accompanying constants are listed in Table 1.

Model selection was based on (i) the value of the goodness of fit parameter WSOS/DF, and (ii) the standard

deviations of calculated log K_s, which were required to satisfy the criterion $\sigma_{\log K} \leqslant 0.15$. A goodness of fit parameter value of 0.1–20 was taken as being indicative of good agreement between model and experiment (Herbelin and Westall, 1994). The *F*-test (Hamilton, 1965), was used to evaluate the significance of a decrease in the goodness of fit parameter due to the inclusion of additional species.

Table 1
Solution phase species included in FITEQL calculations[a]

Dissociation of H_2O	
OH^-	−13.78
Potassium	
KNO_3	0.20
Nickel	
$NiNO_3^+$	0.51
$Ni(NO_3)_2$	−0.01
$NiOH^+$	−9.79
$Ni(OH)_2$	−19.01
$Ni(OH)_3^-$	−29.89
$Ni(OH)_4^{-2}$	−43.56
Ni_2OH^{+3}	−9.71
$Ni_4(OH)_4^{+4}$	−25.97
Copper	
$CuNO_3^+$	0.61
$Cu(NO_3)_2$	−0.44
$CuOH^+$	−7.39
$Cu(OH)_2$	−16.21
$Cu(OH)_3^-$	−26.79
$Cu(OH)_4^{-2}$	−39.16
$Cu_2(OH)_2^{+2}$	−9.92
Zinc	
$ZnNO_3^+$	0.51
$Zn(NO_3)_2$	−0.31
$ZnOH^+$	−8.89
$Zn(OH)_2$	−17.88
$Zn(OH)_3^-$	−27.99
$Zn(OH)_4^{-2}$	−40.06
Zn_2OH^{+3}	−8.01
Cadmium	
$CdNO_3^+$	0.61
$Cd(NO_3)_2$	0.19
$CdOH^+$	−9.97
$Cd(OH)_2$	−20.37
$Cd(OH)_3^-$	−33.19
$Cd(OH)_4^{-2}$	−46.91
Cd_2OH^{+3}	−8.40
$Cd_4(OH)_4^{+4}$	−31.08
Lead	
$PbNO_3^+$	1.28
$Pb(NO_3)_2$	1.39
$PbOH^+$	−7.49
$Pb(OH)_2$	−17.11
$Pb(OH)_3^+$	−27.99
$Pb(OH)_4^{-2}$	−39.26
Pb_2OH^{+3}	−5.37
$Pb_3(OH)_4^{+2}$	−23.44
$Pb_4(OH)_4$	−18.23
$Pb_6(OH)_8^{+4}$	−41.83

[a] All data are listed for I = 0.1 M.

2.4. Model validation

From the literature, a number of studies investigating metal adsorption by MnO_2 were identified (Table 5). Using adsorption parameters determined in this work, together with experimental conditions reported in the selected studies, experimental systems were simulated using MINTEQA2 (Allison et al., 1991). Adsorption constants were corrected to the background electrolyte concentrations employed in the original studies. Activity coefficients were obtained from Dzombak and Morel (1990). The surface area was fixed at 331m^2 g^{-1} in all simulations. This value was used in deriving adsorption constants from the potentiometric data. Simulation conditions were kept as close to reported experimental conditions as possible. In all cases the aqueous phase concentration of the adsorbing metal at equilibrium was maintained within the range reported in the specific study being simulated.

Simulated and literature data sets were compared (i) on a visual basis, i.e. adsorption isotherms or pH dependent pH edges were compared and (ii) in terms of adsorption capacities. Adsorption capacities were calculated by plotting both simulated and literature data according to the linearised Langmuir equation [Eq. (3)], as given by Loganathan and Burau (1973),

$$c(x/m)^{-1} = (ab)^{-1} + ca^{-1} \quad (3)$$

where c is the metal concentration in solution at equilibrium (mM), (x/m) is the metal adsorbed (mmol g^{-1}), a is the maximum adsorption capacity (mmol g^{-1}) and b is a parameter related to the energy of sorption. Linear regression of $c(x/m)^{-1}$ vs c yielded a^{-1}, from which adsorption capacity was calculated. Data sets utilised for model validation are summarised in Table 3.

3. Results

3.1. Alkalimetric titrations

Suspension titrations took ca. 16 h to complete. The equilibrium criterion of $\Delta EMF \leqslant 1.2$ mV h^{-1} was not satisfied at all points in the region $6 < pH < 8$. In general, titrations were reproducible to within 0.2 pH units, with maximum deviation occurring at approximately pH 10. The observed variability is independent of sample age, suggesting that surface modification due to sample ageing did not occur. This agrees with the findings of Stroes-Gascoyne et al. (1987) who observed

Table 2
Proton sorption parameters for δ-MnO_2

	Log K (standard deviation)	
	Homogeneous	Heterogeneous
$\equiv XO^-$	−2.40 (0.13)	−1.27 (0.02)
$\equiv YO^-$	n/a	−5.99 (0.04)
$\equiv YOH_2^+$	n/a	3.52 (0.03)
[XOH]/mol g^{-1}	2.45×10^{-3}	2.23×10^{-3}
[YOH]/mol g^{-1}	n/a	7.66×10^{-4}
Sites nm^{-2}	4.5	5.5
WSOS/DF	64.8	1.8
Data points	240	
pH range	3.2–11.5	

no changes in the surface characteristics of a sample prepared according to the redox method after a storage period of 4 years. Observed variability of the titrations is difficult to assess since this aspect is frequently not addressed in the literature. However, potentiometrically measured Point of Zero Charge (PZC) values for δ-MnO_2 are reported with error estimates of 0.2–0.3 pH units (Morgan and Stumm, 1964; Balistrieri and Murray, 1982; Catts and Langmuir, 1986), which indicates that the reproducibility of titrations is of the order observed in the present study. Similar errors were reported for rutile PZC data (Bérubé and de Bruyn, 1968).

3.2. Adsorption parameters

3.2.1. Surface protonation

Acid-base titration data were evaluated assuming a homogeneous surface consisting of equivalent, amphoteric binding sites, according to the following reaction scheme:

$$\equiv XOH + H^+ \rightleftharpoons \equiv XOH_2^+$$
$$\equiv XOH \rightleftharpoons \equiv XO^- + H^+$$

FITEQL failed to solve the mass balance equations for this model. Surface site concentration [≡XOH] and log K for the reaction $\equiv XOH \rightleftharpoons \equiv XO^- + H^+$ converged but log K for the diprotonated surface species did not converge. This failure is caused by the species $\equiv XOH_2^+$ not occurring in the pH range of 3.2–11 investigated in the present study. It will only be a significant species below the solid's PZC. Evaluation of titration data according to Eq. (2) shows that the δ-MnO_2 sample is negatively charged at pH greater than 3, suggesting a PZC below pH 3. Optimization was successful with the reaction $\equiv XOH + H^+ \rightleftharpoons \equiv XOH_2^+$ discarded. Results are listed in Table 2 and presented graphically in Fig. 2. It is evident that this model is not successful in describing the experimental data.

A heterogeneous surface reaction scheme, which assumes a surface consisting of 2 non-equivalent classes of amphoteric binding sites, was investigated next. Acid-base equilibria were represented by the following reaction scheme:

$$\equiv XOH \rightleftharpoons \equiv XO^- + H^+$$

$$\equiv YOH + H^+ \rightleftharpoons \equiv YOH_2^+$$

$$\equiv YOH \rightleftharpoons \equiv YO^- + H^+$$

The reaction $\equiv XOH + H^+ \rightleftharpoons \equiv XOH_2^+$ was excluded for the reasons discussed earlier. Optimised parameters are summarised in Table 2 and presented graphically in Fig. 2. The improvement brought about by the multi-site model, compared with the single-site model, in describing experimental data is reflected by the improved goodness of fit parameter and the improved agreement between the model and experiment.

Direct comparison of results in Table 2 with literature values is not possible. To our knowledge, diffuse double layer protonation constants for δ-MnO_2 have not previously been reported. To compare the present results with those in the literature, the triple layer model parameters published by Catts and Langmuir (1986) and Fu et al. (1991) were used to simulate titration data with MINTEQA2 (Allison et al., 1991). Diffuse double layer parameters were calculated from these simulated titration

Table 3
Diffuse double layer constants for metal adsorption by δ-MnO_2

	Log K (standard deviation)			
	Copper	Nickel	Zinc	Cadmium
$\equiv XOM^+$	−1.31 (0.06)	−1.65 (0.04)	−1.62 (0.04)	−1.60 (0.02)
$\equiv YOM^+$	−0.20 (0.07)	−1.63 (0.11)	−2.39 (0.23)	−4.32 (0.07)
≡YOMOH	−4.37 (0.09)	−6.08 (0.10)	−7.16 (0.13)	–
≡XOMOH	−3.01 (0.08)	−3.70 (0.08)	−3.95 (0.06)	–
WSOS/DF	0.5	0.5	0.5	0.9
Data points	183	178	120	168
pH range	2.97–9.85	3.04–9.74	3.04–9.80	3.02–9.98

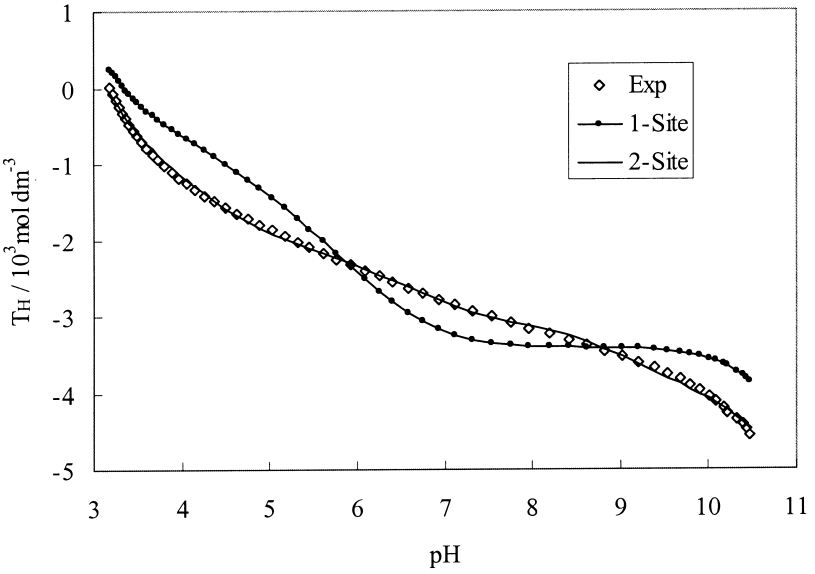

Fig. 2. Comparison of experimental protonation data with calculated results.

curves. Log K values of -2.65 (Catts and Langmuir, 1986) and -2.61 (Fu et al., 1991) for the formation of $\equiv XO^-$, together with a binding site concentration of 3 sites nm^{-2} for both data sets, were found. In these calculations, surface areas of 290 and 296 m^2 g^{-1} reported in the original papers, were used. Goodness of fit parameters of 100 and 91, respectively, were obtained. These results are similar to those obtained from the authors' experimental data using the homogeneous surface assumption.

Application of the heterogeneous model to the data of Catts and Langmuir (1986), yielded values of log $K_1 = -1.36$, log $K_2 = -5.10$ and log $K_3 = 3.04$, with a total binding site concentration of 4 sites nm^{-2} and WSOS/DF = 0.4. This is in good agreement with protonation parameters determined in this study. In order to obtain convergence with the data set of Fu et al. (1991), it was necessary to fix adsorption constants at the values shown in Table 2 and to optimise site concentrations only. This yielded an estimate for the total binding site concentration of 4 sites nm^{-2} with WSOS/DF = 6, indicating an improved fit of the data, compared with the one site model. The parameters are also in reasonable agreement with results from the current study. The heterogeneous surface site model thus provides a significantly better description of experimental data than the homogeneous surface model.

Surface speciation predicted by the heterogeneous surface model is shown in Fig. 3. All species are present at levels of 25% or more, expressed in terms of total site concentration. The surface species $\equiv XO^-$ dominates over the pH range investigated. The speciation of the second site type is dominated by the species $\equiv YOH$ and $\equiv YOH_2^+$ in the lower pH range with $\equiv YO^-$ becoming significant at pH values greater than 6.

3.2.2. Metal adsorption

The surface complexation parameters for Ni, Cu, Zn and Cd are best discussed separately from Pb because the latter exhibited behaviour different from that observed with the others.

3.2.2.1. Ni, Cu, Zn and Cd surface complexation. Adsorption constants and accompanying surface species are summarised in Table 3. Models consisting of the same surface species were required to fit Cu, Zn and Ni data. Cadmium did not require the inclusion of hydroxy surface species. Constants for Cu, Ni and Zn obey the Irving–Williams stability sequence (Irving and Williams, 1948, 1953). Adsorption constants for Ni, Cu and Zn by Fe oxides also conform to this stability sequence (Stumm, 1992).

3.2.2.2. Lead. Results for Pb are summarised in Table 4. The model consisting of a dinuclear Pb hydroxide surface species, $\equiv XOPb_2OH^{2+}$, which forms according to the reaction $\equiv XOH + 2Pb^{2+} + H_2O \rightleftharpoons \equiv XOPb_2OH^{2+} + 2H^+$, was selected as the model for Pb adsorption based on the lowest goodness of fit parameter. The selection of this species is supported by spectroscopic evidence provided by Manceau et al. (1992c), who investigated Pb adsorption by Birnessite in situ using EXAFS spectroscopy. They found evidence for multi-nuclear surface complexes with Pb oxy/hydroxy-like local structure coordinated with Birnessite edges. Similar observations for Pb adsorption by γ-Al_2O_3

were made by Chisholm-Brause et al. (1990), also using EXAFS. Although this model is capable of describing the adsorption data, the fit obtained is not entirely satisfactory. Therefore, adsorption data were also modelled with mononuclear surface complexes (Table 4) but none of the models evaluated were more successful than the dinuclear surface complex model.

3.3. Model validation

3.3.1. Adsorption sequence of metals

Modelling results show that the metal adsorption sequence depends on pH and metal : binding site concentration ratio. For a metal : binding site ratio of 1 : 30 and pH 4, a sequence Pb ≈ Cu > Ni ≈ Zn > Cd is predicted. At pH 6 and 8, 100% adsorption is observed and therefore an adsorption sequence can not be determined. For a metal : binding site ratio of 1 : 3, a sequence of Cu > Pb > Ni > Zn > Cd is predicted at pH 4 and Cu ≈ Pb ≈ Ni ≈ Zn > Cd is predicted for pH 6 and 8. Modelling results agree with the observations that Pb and Cu are adsorbed preferentially (Gadde and Laitinen, 1974; Balikungeri and Haerdi, 1988; McKenzie, 1989; Fu et al., 1991). For Zn, Cd and Ni some confusion is evident, with Zasoski and Burau (1988) and Gadde and Laitinen (1974) reporting Zn > Cd while Balikungeri and Haerdi (1988) reverse the order. Gray and Malati (1979) report Zn ≈ Cd > Ni, which is contrary to expectations, based on the Irving–Williams stability sequence. Thus, in broad terms, modelling results correspond with trends observed experimentally. However, some of the observed adsorption sequences are doubtful if evaluated against the well-proven Irving-Williams stability sequence.

3.3.2. Copper

Model prediction of the pH-dependent Cu adsorption data of Catts and Langmuir (1986) and Fu et al. (1991) is shown in Fig. 4. Reasonable agreement between simulated and experimental results is observed.

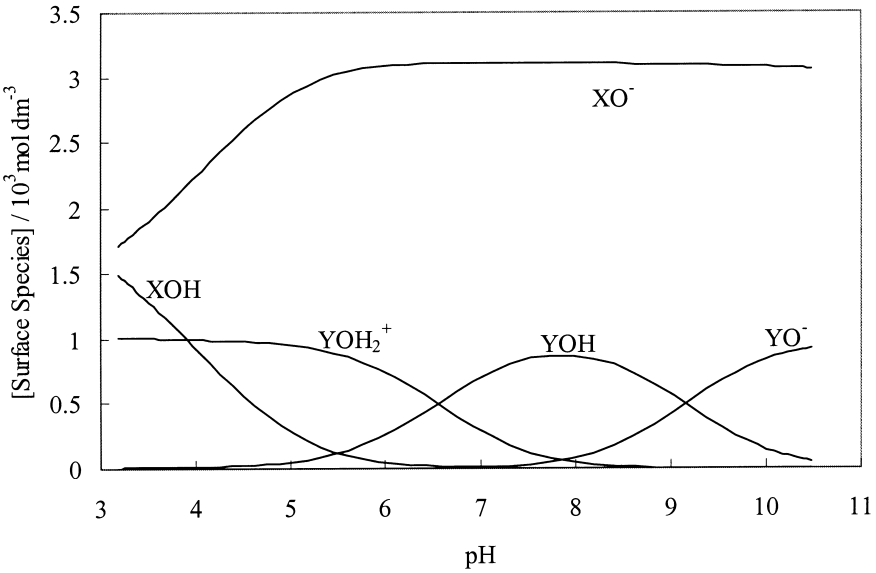

Fig. 3. Surface speciation as a function of pH as predicted by the 2-surface site protonation model.

Table 4
Lead adsorption constants for the formation of a multinuclear surface complex

Species			Log K (standard deviation)			
$\equiv XOM_2OH^{+2}$	−1.49 (0.03)					
$\equiv XOM^{+}$		−0.55 (0.03)	−0.59 (0.07)	−1.09 (0.05)	−1.04 (0.05)	
$\equiv YOM^{+}$			−0.57 (0.43)		−1.21 (0.14)	
$\equiv XOMOH$				−2.38 (0.03)	−2.87 (0.03)	−2.68 (0.02)
WSOS/DF	1.1	7.2	1.8	1.9	1.8	2.7
Data points			165			
pH range			3.00–9.85			

Simulated data show a sharp decrease in dissolved Cu in the pH range 4–5, indicating a sharp rise in Cu adsorbed. The experimental curve exhibits a more gradual change suggesting a gradual increase in adsorption over the pH range investigated.

Simulated Cu adsorption isotherms at pH 5.5 and 6 are compared with experimental data collected by Fu et al. (1991) and Stroes-Gascoyne (1983) in Fig. 5. At pH 5.5, the simulated isotherm overestimates observed adsorption over the Cu concentration range investigated by a constant difference of approximately 1 mmol g^{-1}. At pH 6, agreement between model predictions and experimental observations is well within experimental variability. Stroes-Gascoyne (1983) investigated Cu adsorption by (a) three δ-MnO_2 samples prepared according to the same preparation scheme (sets A, B,

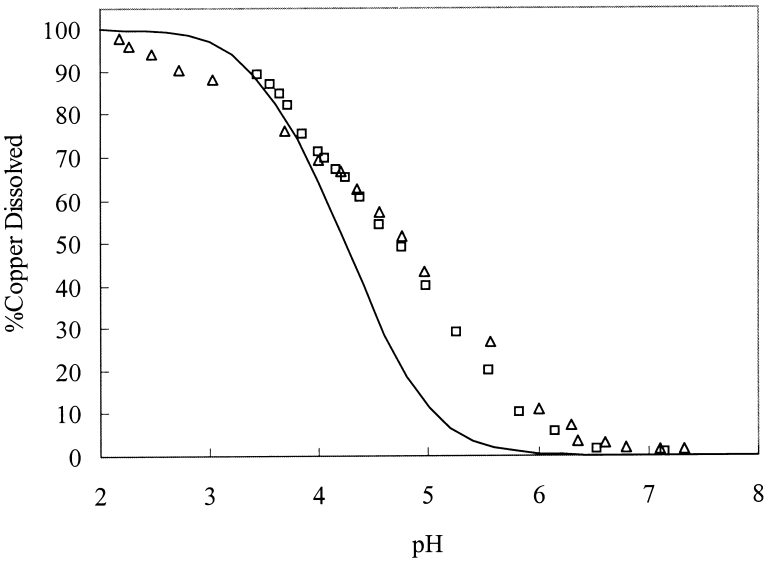

Fig. 4. Comparison between experimental and simulated pH-dependent Cu adsorption data (— model; Δ Catts and Langmuir, 1986; □ Fu et al., 1991).

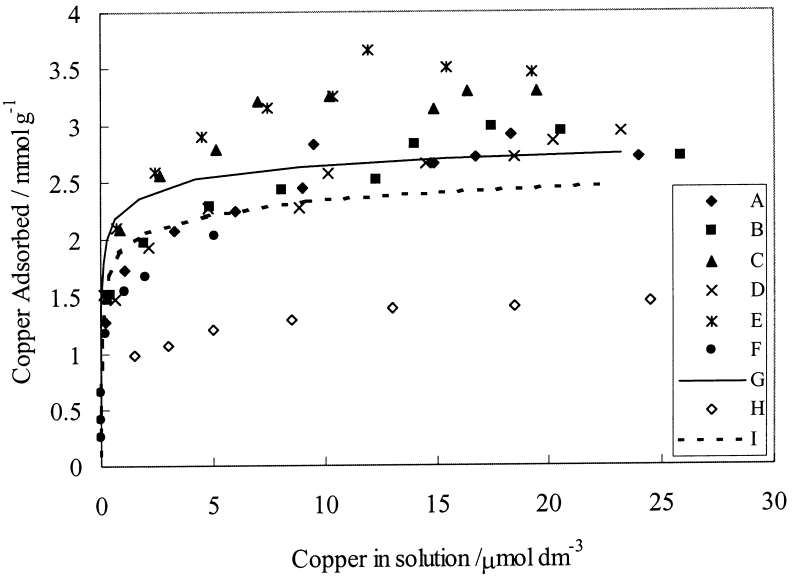

Fig. 5. Comparison between simulated and experimental Cu adsorption isotherms collected at pH 5.5 (H: Fu et al., 1991; I: model) and pH 6 (G: model; A to F: Stroes-Gascoyne, 1983 and Stroes-Gascoyne et al., 1987).

and F, Fig. 5) and (b) replicate adsorption experiments using the same batch of solid (sets C, D and E, Fig. 5). The significant variability observed in these results highlights the difficulty in obtaining reproducible results for metal adsorption by MnO_2.

It is interesting to note that the simulated isotherms exhibit only a small increase in metal adsorbed in going from pH 5.5 to 6. By considering the pH dependent adsorption curve (Fig. 4) determined by Fu et al. (1991), together with the total Cu concentration of 8×10^{-5} M employed, a solution concentration of Cu of ca. 5 μmol dm^{-3} and an adsorbed concentration of 1.5 mmol g^{-1} is obtained at pH 6. Corresponding values ranging from 2 to 2.7 mmol g^{-1} are obtained from the Stroes-Gascoyne isotherm (Fig. 5). This suggests that the solid used by Fu et al. (1991) sorbs significantly less Cu than was observed by Stroes–Gascoyne (1983) and serves as a further illustration of the variability observed in experimental studies of metal adsorption by δ-MnO_2 from different laboratories.

In Table 6 experimental and simulated Cu adsorption capacities are compared. Good agreement is observed with the data of Stroes–Gascoyne (1983) and Balikungeri and Haerdi (1988). The agreement with the data of Stroes–Gascoyne (1983) is particularly encouraging, since these data are extensive. Also, the solid preparation procedure followed by us is similar to that used by Stroes–Gascoyne (1983). However, for the Fu et al. (1991) data, poorer agreement between model and experiment was obtained.

3.3.3. Nickel

Only the data of Gray and Malati (1979) were available for model validation. Fig. 6 shows a comparison between the literature and model predictions. Compared with the experimental data set, the model overestimates Ni adsorption significantly.

3.3.4. Zinc

For Zn, data sets at pH 4, 6 and 8 are available. Data at pH 4 originate from the laboratory of Burau and were collected under similar conditions, except that Zasoski and Burau (1988) employed lower metal concentrations than Loganathan and Burau (1973). Good agreement with the data set of Zasoski and Burau (1988) is observed (Fig. 7). Compared with the Loganathan and Burau (1973) data, simulated Zn adsorbed overestimates experimental values. Although only a limited number of points overlap, the trend exhibited by the Zasoski and Burau (1988) data suggests more Zn adsorbed than does the Loganathan and Burau (1973) data.

A comparison of the experimental data of Gray and Malati (1979) and Zasoski and Burau (1988) with simulated data is shown in Fig. 8. Better agreement is observed between simulated data and the data of Zasoski and Burau (1988) than with the data of Gray and Malati (1979). However, in both cases the model overestimates Zn adsorption. In Fig. 9, simulated pH dependent Zn adsorption data is compared with the data of Catts and Langmuir (1986). Experimental

Table 5
Metal adsorption data sets used for the purpose of validating the adsorption models proposed for δ-MnO_2

Metal	Data set	Remarks
Ni	Gray and Malati, 1979	• pH 6 isotherm and adsorption capacity.
Cu	Catts and Langmuir, 1986	• pH dependent sorption.
	Stroes-Gascoyne et al. 1987 Stroes-Gascoyne, 1983	• pH 6 isotherm; binding capacity at this pH for different preparations.
	Balikungeri and Haerdi, 1988	• Binding capacities at pH 5.5, 6.0 and 6.5.
	Fu et al., 1991	• pH dependent sorption; pH 5.5 isotherm and binding capacity
Zn	Loganathan and Burau, 1973	• sorption isotherm at pH 4; Langmuir plot; adsorption capacity.
	Gadde and Laitinen, 1974	• pH 6 isotherm and adsorption capacity.
	Gray and Malati, 1979	• pH 6 isotherm and adsorption capacity.
	Catts and Langmuir, 1986	• pH dependent sorption.
	Zasoski and Burau, 1988	• adsorption data at pH 4, 6 and 8 (limited); binding capacities at different pHs.
Cd	Gadde and Laitinen, 1974	• pH 6 isotherm and adsorption capacity.
	Gray and Malati	• pH 6 isotherm and adsorption capacity
	Zasoski and Burau, 1988	• adsorption data at pH 4, 6 and 8 (limited); binding capacities at different pHs.
	Balikungeri and Haerdi, 1988	• Binding capacities at pH 5.5, 6.0 and 6.5.
	Fu et al., 1991	• pH dependent sorption; isotherms at pH 5.5, 7.0 and 8; binding capacities.
Pb	Gadde and Laitinen, 1974	• pH 6 isotherm and adsorption capacity.
	Catts and Langmuir, 1986	• pH dependent sorption.
	Balikungeri and Haerdi, 1988	• Binding capacities at pH 5.5, 6.0 and 6.5.

Table 6
Comparison between calculated and experimental adsorption capacities for copper, zinc and cadmium by δ-MnO_2

Metal	pH	I (M)	Adsorption capacity (mmol g^{-1})		Source
			Exp	Model	
Cu	5.5	0.01	1.54	2.64	Fu et al., 1991
		0.1	2.40	2.39	Balikungeri and Haerdi, 1988
	6.0	0.01	2.2-3.0	2.77	Stroes-Gascoyne et al., 1979;1987
		0.1	3.20	2.65	Balikungeri and Haerdi, 1988
	6.5	0.1	3.00	2.80	Balikungeri and Haerdi, 1988
Zn	4.0	0.001	1.00	1.30	Loganathan and Burau, 1973
		0.001	0.70	0.70	Zasoski and Burau, 1988
	6.0	0.1	0.47	2.16	Balikungeri and Haerdi, 1988
		0.01	1.51	2.70	Gray and Malati, 1979
		0.001	1.96	2.50	Zasoski and Burau, 1988
		[a]	2.80	2.2-2.7	Gadde and Laitinen, 1974
	6.5	0.1	1.15	2.48	Balikungeri and Haerdi, 1988
Cd	4.0	0.001	0.83	0.60	Zasoski and Burau, 1988
	5.5	0.01	0.43	0.85	Fu et al., 1991
		0.1	0.62	0.65	Balikungeri and Haerdi, 1988
	6.0	0.001	1.40	1.20	Zasoski and Burau, 1988
		0.01	1.21	1.17	Gray and Malati, 1979
		0.1	0.93	0.81	Balikungeri and Haerdi, 1988
		a	1.95	0.8-1.2	Gadde and Laitinen, 1974
	6.5	0.1	0.93	1.00	Balikungeri and Haerdi, 1988
	7.0	0.01	1.20	1.15	Fu et al., 1991
	8.0	0.01	2.12	1.58	Fu et al., 1991

[a] Ionic strength not stated in original reference, assumed 0.1 M.

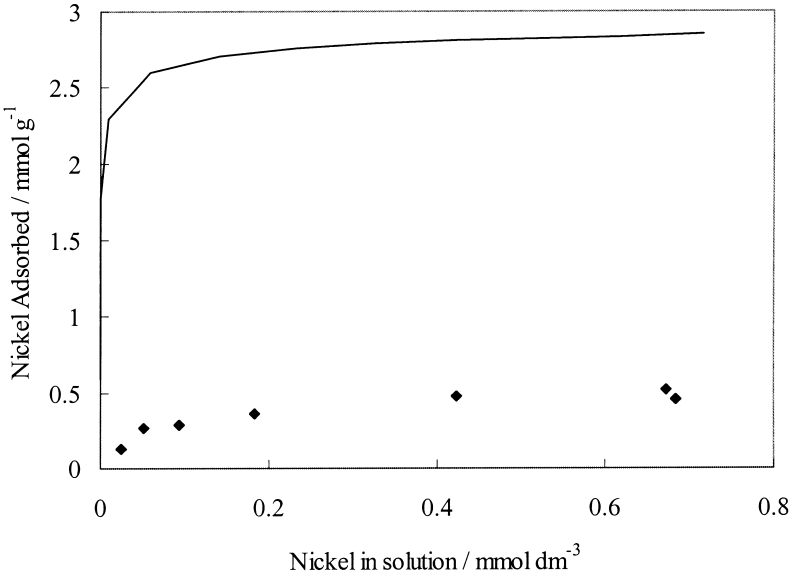

Fig. 6. Comparison between a simulated and an experimental Ni adsorption isotherm collected at pH 6 (— model; ◆ Gray and Malati, 1979).

results are predicted well up to pH ca. 4 but Zn adsorption is overestimated at higher pH. Adsorption capacities calculated from experimental and simulated data sets are compared in Table 6. Calculated and observed adsorption capacities agree well at pH 4. At higher pH, poorer agreement is observed.

3.3.5. Cadmium

In Fig. 10, pH dependent adsorption data of Fu et al. (1991) is compared with simulated data. Cadmium adsorption is consistently overestimated by the model. In Fig. 11, simulated adsorption results are compared with data sets obtained at pH 4 (Zasoski and Burau,

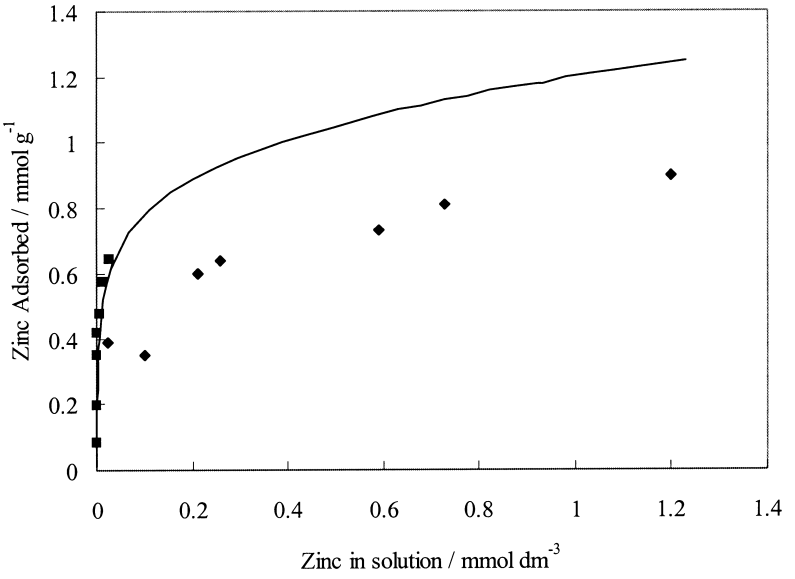

Fig. 7. Comparison between simulated and experimental Zn adsorption isotherms collected at pH 4 (— model; ◆ Loganathan and Burau, 1973; ■ Zasoski and Burau, 1988).

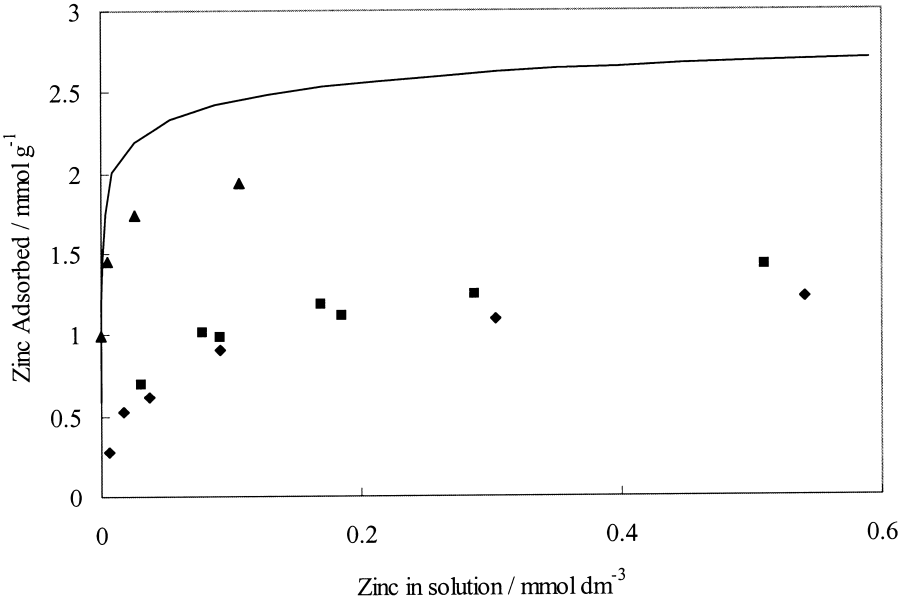

Fig. 8. Comparison between simulated and experimental Zn adsorption isotherms collected at pH 6 (— model; ▲ Zasoski and Burau, 1988; ■ Gray and Malati (308K), 1979; ◆ Gray and Malati (293K), 1979).

1988) and at pH 5.5, 7 and 8 (Fu et al. 1991). Best agreement between model and experiment is observed for the pH 7 data. For the pH 4 data, adsorption is underestimated by the model while for the pH 5.5 data set, the model overestimates adsorption. There is, however, an anomaly between the results reported by Fu et al. (1991) at pH 5.5 and those of Zasoski and Burau (1988) at pH 4. It is evident that Cd_{ads} (pH4) > Cd_{ads} (pH5.5) by approximately a factor of 2. This may be due to the pH 4 study being carried out at an ionic strength of 0.001 M while the pH 5.5 study was carried out at 0.01 M. It may, however, be expected that the increase in pH will negate the negative effect of an increase in ionic strength on adsorption. Good agreement between simulated and experimental data sets is observed at pH 6 (Fig. 12).

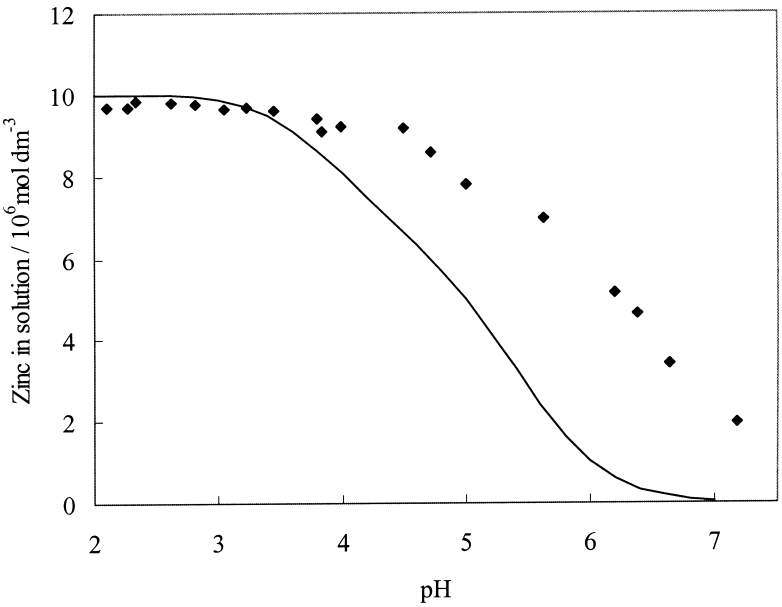

Fig. 9. Comparison between experimental and simulated pH-dependent Zn adsorption data (— model; ◆ Catts and Langmuir, 1986).

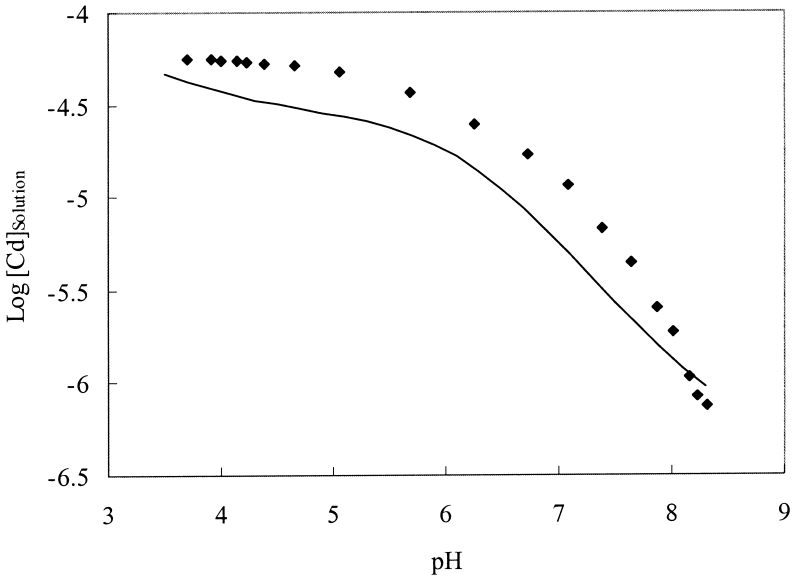

Fig. 10. Comparison between experimental and simulated pH-dependent Cd adsorption data (— model; ◆ Fu et al., 1991).

Adsorption capacities obtained from experimental and simulated results are shown in Table 6. In general, good agreement between adsorption capacities obtained from experimental observations with those obtained from simulated adsorption data, is observed. Exceptions are the Fu et al. (1991) data set at pH 5.5 and pH 8, where the model provides an over- and an under-estimation of the respective adsorption capacities. However, as discussed above, the results of Fu et al. (1991) at pH 5.5 seem low when compared with the result obtained by Zasoski and Burau (1988) at pH 4.

3.3.6. Lead

A limited number of Pb adsorption data sets are available for model validation purposes. In Fig. 13, simulated pH dependent adsorption data are compared

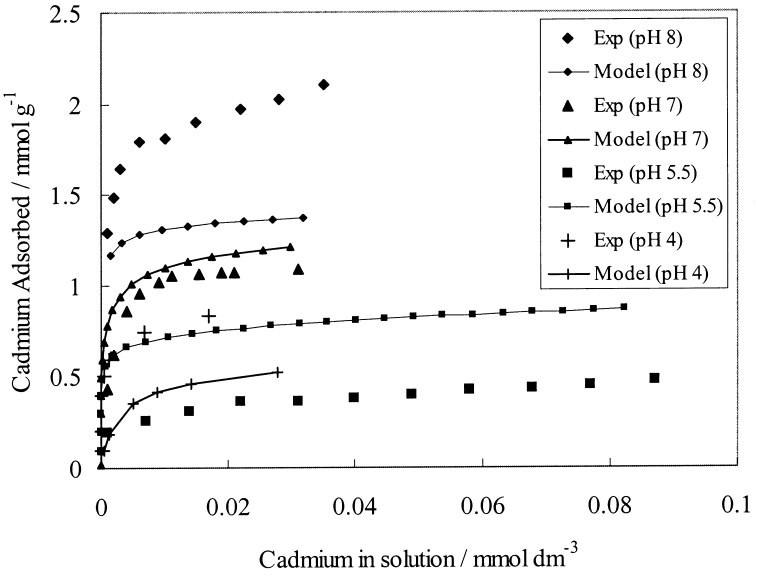

Fig. 11. Comparison between simulated and experimental Cd adsorption isotherms collected at pH 4 (Zasoski and Burau, 1988), pH 5.5, pH 7 and pH 8 (Fu et al., 1991).

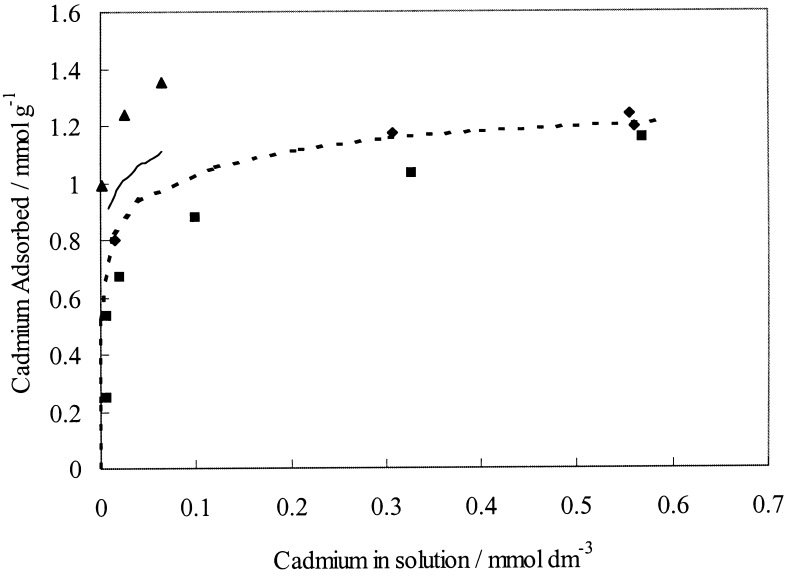

Fig. 12. Comparison between simulated and experimental Cd adsorption isotherms collected at pH 6 (▲ Zasoski and Burau, 1988; — model; Gray and Malati, 1979 (■ 308K, ◆ 293K, ··· model).

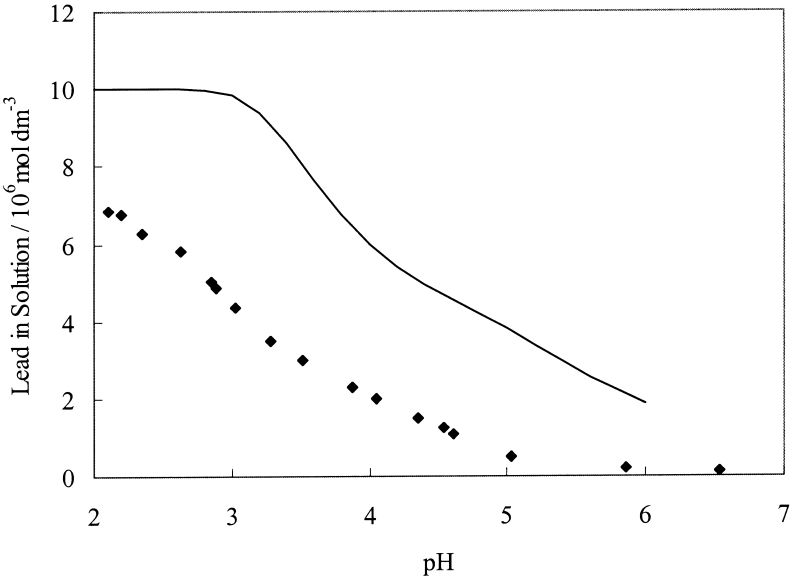

Fig. 13. Comparison between experimental and simulated pH-dependent Pb adsorption data (— model; ◆ Catts and Langmuir, 1986).

with the experimental data of Catts and Langmuir (1986). The model underestimates Pb adsorption (i.e. overestimates Pb in solution) by approximately a factor of 2–3. Gadde and Laitinen (1974) reported a Pb adsorption isotherm obtained at pH 6. They found that Pb adsorption increases monotonically instead of exhibiting a plateau, indicative of maximum sorption capacity being reached. They calculated an adsorption capacity of 6.4 mmol g^{-1} from their data. This value is, however, thought to be unrealistic and most probably included a Pb precipitate. Equilibrium simulations of their experimental system show that, allowing equilibrium with atmospheric CO_2, a number of Pb carbonate solids would be present at supersaturated levels. Since they do not mention any steps aimed at excluding CO_2 from their experiments, the possibility of Pb precipitates contributing to their results cannot be excluded. Therefore, their results were ignored.

4. Discussion

The present adsorption model differs from earlier ones in respect of the heterogeneous surface assumption employed. The concept of different classes of surface hydroxyl groups has been proposed and illustrated before by a number of workers for a variety of solids (e.g. Schindler and Stumm, 1987; Hiemstra et al., 1989; Barrow, 1993; Contescu et al., 1993, 1994; Rustad et al., 1996). It may be explained by considering the coordinative environments of metal ions and surface hydroxyl groups in hydrated surfaces. Surface hydroxyls may be present as bridging and terminal groups and metal centres may be coordinated with two or more hydroxyls. These differing configurations will give rise to terminal hydroxyls of different acidity. Since these studies were not carried out on MnO_2, they do not provide proof for a heterogeneous surface for this solid. They do, however, provide support for the assumption of surface heterogeneity. Binding sites belonging to different chemical classes may also be rationalised in terms of the limited information available on the structure of δ-MnO_2. Manceau et al. (1992a,b), based on XANES and EXAFS studies, express the opinion that δ-MnO_2 should be pictured as a "3-D (O,OH) framework where cubic and hexagonal close-packing arrangements alternate at random and where octahedral sites are randomly filled, but where two adjacent $Mn(O,OH)_6$ octahedra cannot share faces". According to these workers, the δ-MnO_2 structure "probably consists of a mosaic of single and multiple octahedral chains having variable length and width". They provide evidence that links the δ-MnO_2 structure with the Todorokite tunnel structure. On the basis of this proposed non-uniform structure, hydroxyl groups of differing reactivity is perhaps a more realistic expectation than sites of uniform reactivity.

Some of the surface species invoked in the description of metal adsorption data may be criticised on the grounds that, at pH values where they are postulated to be present as surface complexes, they have a very low abundance in the solution phase. This would be the case for all the ≡XOMOH species. These hydroxy species are present in solution, albeit at quite low concentrations especially in the lower pH ranges. The solid surface acts as a sink for these species by adsorbing them and thereby removing them from solution. According to Le

Chatelier's principle, the system will respond to this disturbance of equilibrium by shifting the equilibrium in a direction that favours the species being consumed. Furthermore, the EXAFS results of Manceau et al. (1992c), which provided evidence for the existence of polynuclear Pb oxy/hydroxide surface complexes, were collected at pH 3. Furthermore, certain criteria exist which may be used as safeguards (but not guarantees) against mistakenly selecting species that arise from errors in the data set. These criteria originate from speciation studies in solution chemistry. Baes and Mesmer (1976) require that an equilibrium constant be larger than or equal to 3 times its standard deviation, σ_K, before accepting a species as significant. In logarithmic terms, this is equal to $\sigma_{LogK} \leqslant 0.15$. Dzombak and Morel (1990), in their work on hydrous ferric oxide applied this criterion to assist them in species selection. Sillén (as referenced by Baes and Mesmer), requires a less stringent criterion of an equilibrium constant being larger than or equal to $1.5\sigma_K$, which is equal to $\sigma_{LogK} \leqslant 0.29$. The log *K*s for most of the species postulated in this work satisfy the criterion of Baes and Mesmer (1976), with the exception of $\equiv YOZn^+$, which satisfies the criterion of Sillén. Other workers (e.g. Kramer, 1988) require species to be present at levels of at least 5% of total metal and total ligand. In the current study, all species postulated are present at levels of more than 5% of the total metal concentration employed. This criterion is not always satisfied when species abundance is expressed in terms of total binding site concentration because of the metal to total binding site ratio of approximately 1:10 employed in this work.

The accuracy of the constants is difficult to assess. According to Martell and Motekaitis (1988), "absolute accuracy, even though it is difficult to obtain, always requires a carefully calibrated pH meter-electrode system, a low σ_{Fit}, the assurance that the stoichiometric variables are accurate, and the presence of a substantial proportion of each species in the equilibrium expression under the conditions of the experiment". In the present work, most of these criteria are satisfied. However, due to the paucity of structural information regarding the surface (and therefore about binding site characteristics), the accuracy of stoichiometric variables is difficult to assess. Furthermore, binding site concentrations were calculated from protonation data and no independent techniques were used to assess these concentrations. It is, however, not possible to quantify the effects of these uncertainties on the modelling parameters presented.

Model validation results indicate reasonable agreement between experimental studies and simulation results in a number of cases. In general, the discrepancy between simulated and experimental results is also reflected in experimental results emanating from different laboratories. This suggests a fundamental difficulty in obtaining reproducible results for adsorption studies involving the MnO_2 surface. Nevertheless, the model presented here has usefulness in studying the surface processes of MnO_2 solids and may be used together with the Diffuse Double Layer surface parameters of Dzombak and Morel (1990) to more realistically model the effect of particulate material on the fate of metals in natural systems.

Acknowledgements

P.J.P. acknowledges financial support from CSIR. P.W.L. acknowledges financial support from the Foundation for Research Development and the University of Cape Town.

References

Adams, W.J., Kimberle, R.A., Barnett, J.W., 1992. Sediment quality criteria and aquatic life assessment. Environ. Sci. Technol. 26, 1864–1875.

Allison, J.D., Brown, D.S., Novo-Gradac, K.J., 1991. MINTEQA2/PRODEFA2, a geochemical assessment model for environmental systems: version 3.0 user's manual. EPA/600/3-91/021.

Baes, C.F., Mesmer, R.F., 1976. The Hydrolysis of Cations. John Wiley and Sons, New York.

Balikungeri, A., Haerdi, W., 1988. Complexing abilities of hydrous manganese oxide surfaces and their role in the speciation of heavy metals. Int. J. Environ. Anal. Chem. 34, 215– 225.

Balistrieri, L.S., Murray, J.W., 1982. The surface chemistry of δ-MnO_2 in major ion sea water. Geochim. Cosmochim. Acta 46, 1041–1052.

Barrow, N.J., 1993. Effects of surface heterogeneity on ion adsorption by metal oxides and by soils. Langmuir 9, 2606–2611.

Bassett, R.L., Melchior, D.C., 1990. Chemical modelling of aqueous systems: an overview. In: Melchior, D.C., Bassett, R.L. (Eds), Chemical Modelling of Aqueous Systems II., ACS Symposium series 416, Chapter 1. American Chemical Society, pp. 1–14.

Bérubé, Y.G., de Bruyn, P.L., 1968. Adsorption at the rutile-solution interface. I. Thermodynamic and experimental study. J. Colloid Interface Sci. 27, 305–318.

Catts, J.G., Langmuir, D., 1986. Adsorption of Cu, Pb and Zn by δ-MnO_2: applicability of the site binding-surface complexation model. Appl. Geochem. 1, 255–264.

Chisholm-Brause, C.J., Hayes, K.F., Roe, A.L., Brown, G.E., Parks, G.A., Leckie, J.O., 1990. Spectroscopic investigation of Pb(II) complexes at the γ-Al_2O_3/water interface. Geochim. Cosmochim. Acta 54, 1897–1909.

Contescu, C., Jagiello, J., Schwarz, J.A., 1993. Heterogeneity of proton binding sites at the oxide/solution interface. Langmuir 9, 1754–1765.

Contescu, C., Contescu, A., Schwartz, J.A., 1994. Thermodynamics of proton binding at the alumina/aqueous solution interface. A phenomenological approach. J. Phys. Chem. 98, 4327–4335.

Dzombak, D.A., Hayes, K.F., 1992. Comment on "Recalculation, evaluation and prediction of surface complexation constants for metal adsorption on iron and manganese dioxides". Environ. Sci. Technol 26, 1251–1253.

Dzombak, D.A., Morel, F.M.M., 1990. Surface Complexation modelling: Hydrous Ferric Oxide. John Wiley and Sons, New York.

Fu, G., Allen, H.E., Cowan, C.E., 1991. Adsorption of cadmium and copper by manganese oxide. Soil Sci. 152, 72–81.

Gadde, R.R., Laitinen, H.A., 1974. Studies of heavy metal adsorption by hydrous iron and manganese oxides. Anal. Chem. 46, 2022–2026.

Gray, M.J., Malati, M.A., 1979. Adsorption from aqueous solution by δ-Manganese dioxide II. Adsorption of some heavy metal cations. J. Chem. Tech. Biotechnol. 29, 135–144.

Hamilton, W.C., 1965. Significance tests on the crystallographic R factor. Acta Crystallogr. 18, 562–510.

Herbelin, A., Westall, J.C., 1994. FITEQL: a computer program for determination of chemical equilibrium constants from experimental data, version 3.1, Report 94-01, Oregon State University.

Hiemstra, T., van Riemsdijk, W.H., Bolt, G.H., 1989. Multisite proton adsorption modelling at the solid/solution interface of (hydr)oxides: a new approach. 1. Model description and evaluation of intrinsic reaction constants. J. Colloid Interface Sci. 133, 91–104.

Irving, H., Williams, R.J.P., 1948. Order of stability of metal complexes. Nature 162, 746–747.

Irving, H., Williams, R.J.P., 1953. The stability of transition metal complexes. J. Chem. Soc. 3192–3210.

Kramer, U., 1988. Complexation of divalent copper, zinc and calcium ions by phosphate esters in Aqueous Solution. PhD thesis, University of Cape Town, South Africa.

Linder, P.W., Torrington, R.G., Williams, D.R., 1984. Analysis Using Glass Electrodes. Open University Press.

Loganathan, P., Burau, R.G., 1973. Sorption of heavy metal ions by a hydrous manganese dioxide. Geochim. Cosmochim. Acta 37, 1277–1293.

Lyman, W.J., 1995. Transport and transformation. In: Rand, G.M. (Ed.), Fundamentals of Aquatic Toxicology: Effects, Environmental Fate and Risk Assessment, Chapter 15, Taylor Frances, pp. 449–492.

Manceau, A., Gorshkov, A.I., Drits, V.A., 1992a. Structural chemistry of Mn, Fe, Co and Ni in manganese hydrous oxides: part I. Information from XANES spectroscopy. Am. Mineral. 77, 1133–1143.

Manceau, A., Gorshkov, A.I., Drits, V.A., 1992b. Structural chemistry of Mn, Fe, Co and Ni in manganese hydrous oxides: part II. Information from EXAFS spectroscopy and electron and X-ray diffraction. Am. Mineral. 77, 1144–1157.

Manceau, A., Charlet, L., Boisset, M.C., Didier, B., Spadini, L., 1992c. Sorption and speciation of heavy metals on hydrous Fe and Mn oxides. From microscopic to macroscopic. Appl. Clay Sci. 7, 201–223.

Martell, A.E., Motekaitis, R.J., 1988. Determination and Use of Stability Constants. VCH Publishers.

McKenzie, R.M., 1989. Manganese oxides and hydroxides. In: Dixon, J.B., Weed, S.B. (Eds), Minerals in Soil Environments; SSSA Book series 1, Soil Science Society of America, Chapter 9, pp. 439-465.

Morgan, J.J., Stumm, W., 1964. Colloid-chemical properties of manganese dioxide. J. Colloid Interface Sci. 19, 347–359.

Onuki, T., 1990. Adsorption of radioactive cobalt by a mixture of manganese dioxide and montmorrillonite. J. Nucl. Sci. Technol 27, 1068–1071.

Rustad, J.A., Felmy, A.R., Hay, B.P., 1996. Molecular statics calculations of proton binding to goethite surfaces: a new approach to estimation of stability constants for multisite surface complexation models. Geochim. Cosmochim. Acta 60, 1563–1567.

Schindler, P.W., Stumm, W., 1987. The surface chemistry of oxides, hydroxides and oxide minerals. In: Stumm, W. (Ed), Aquatic Surface Chemistry: Chemical Processes at the Particle-Water Interface, Chapter 4 John Wiley and Sons, pp. 83–110.

Shea, D., 1988. Developing national sediment quality criteria. Environ. Sci. Technol. 22, 1256–1261.

Sing, K.S.W., 1985. Reporting physisorption data for gas/solid systems. Pure Appl. Chem. 57, 603–619.

Smith, R.W., Jenne, E.A., 1991. Recalculation, evaluation and prediction of surface complexation constants for iron and manganese oxides. Environ. Sci. Technol. 25, 525–531.

Stroes-Gascoyne, S., 1983. Adsorption behaviour of δ-manganese dioxide in relation to its use as a resin in trace metal speciation studies. PhD thesis, McMaster University, Canada.

Stroes-Gascoyne, S., Kramer, J.R., Snodgrass, W.J., 1987. Preparation, characterization and aging of δ-MnO_2, for use in trace metal speciation studies. Appl. Geochem. 2, 217–226.

Stumm, W., 1992. Chemistry of the Solid-Water Interface. John Wiley and Sons, New York.

Ure, A.M., Davidson, C.M., 1995. Introduction to speciation. In: Ure, A.M., Davidson, C.M. (Eds.), Chemical Speciation in the Environment Chapter 1, Blackie Academic Press, pp. 1–5.

van der Kooij, L.A., van de Meent, D., van Leeuwen, C., Bruggeman, W.A., 1991. Deriving quality criteria for water and sediment from the results of aquatic toxicity tests and product standards: application of the equilibrium partitioning method. Wat. Res. 25, 697–705.

Waite, T.D., 1989. Mathematical modelling of trace element speciation. In: Batley, G.E. (Ed), Trace Element Speciation: Analytical Methods and Problems, Chapter 5, CRC Press, pp. 117–184.

Westall, J.C., Jones, J.D., Turner, G.D., Zachara, J.M., 1995. Models for association of metal ions with heterogeneous environmental sorbents. 1. Complexation of Co(II) by Leonardite humic acid as a function of pH and $NaClO_4$ concentration. Environ. Sci. Technol. 29, 951–959.

Zasoski, R.J., Burau, R.G., 1988. Sorption and sorptive interaction of cadmium and zinc on hydrous manganese oxide. Soil Sci. Soc. Am. J. 52, 81–87.